JOURNAL OF PROPULSION AND POWER
Vol. 21, No. 3, May–June 2005

Effects of Fuel Distribution on Detonation Tube Performance

H. Douglas Perkins*
NASA Glenn Research Center at Lewis Field, Cleveland, Ohio 44135
and
Chih-Jen Sung†
Case Western Reserve University, Cleveland, Ohio 44106

A pulse detonation engine uses a series of high-frequency intermittent detonation tubes to generate thrust. The process of filling the detonation tube with fuel and air for each cycle may yield nonuniform mixtures. Uniform mixing is commonly assumed when calculating detonation tube thrust performance. Detonation cycles featuring idealized nonuniform H_2–air mixtures were analyzed using a two-dimensional Navier–Stokes computational fluid dynamics code with finite-rate chemistry. Mixture nonuniformities examined included axial equivalence ratio gradients, transverse equivalence ratio gradients, and partially fueled tubes. Three different average test section equivalence ratios were studied: one stoichiometric, one fuel lean, and one fuel rich. All mixtures were detonable throughout the detonation tube. Various mixtures representing the same average test section equivalence ratio were shown to have specific impulses within 1% of each other, indicating that good fuel–air mixing is not a prerequisite for optimal detonation tube performance under the conditions investigated in an H_2–air system.

Introduction

THE concept of a pulse detonation engine (PDE) for aerospace propulsion system applications is not new. The work at the University of Michigan in the 1950s is a prime example.[1] However, it was not until repetitive detonations of larger diameter detonation chambers with gaseous hydrocarbon fuels at relatively high frequencies were demonstrated in the mid-1980s that it became apparent that practical devices might be possible. The many advances in PDE technology that have occurred over the past decade, chronicled by Wu et al.,[2] and Kailasanath,[3] among others, have stimulated interest in the mainstream propulsion development community.[4,5] Government and industry organizations are currently developing PDEs and derivative configurations for missions as diverse as missiles, commercial aircraft, and launch vehicles.[6] At the heart of each of these unique propulsion systems is a series of high-frequency intermittent (pulse) detonation tubes.

PDEs are attractive for several reasons. First, Kailasanath and Patnaik,[7] among others, have shown that the thermal efficiency of the detonation cycle can be significantly higher than the thermal efficiency of the standard Brayton cycle found in gas turbine engines and ramjets, 49% vs 27% in an example case where both combustion processes begin at 3-atm pressure. Second, because total pressure increases significantly during detonative combustion, instead of decreasing slightly as in deflagrative combustion, it is possible to decrease the amount of compression required before the combustion process, thus leading to simplified, lighter, lower cost engine architectures. For some missions, such as air-launched missiles, it is possible to eliminate all mechanical precompression and operate the PDE as a "supercharged" ramjet, even at relatively low subsonic Mach numbers. Last, a PDE detonation chamber does not have to be round, nor do the detonation chambers have to be grouped in circular arrays if turbomachinery components have been eliminated, thus, leading to a more aerodynamically efficient airframe integration than with a gas turbine engine.

Received 5 May 2003; revision received 6 December 2004; accepted for publication 9 December 2004.

*Aerospace Engineer, Engine Systems Branch; Hugh.D. Perkins@nasa.gov. Member AIAA.
†Associate Professor, Department of Mechanical and Aerospace Engineering; cjs15@po.cwru.edu. Senior Member AIAA.

It is likely that, in any application of detonative combustion for propulsion, the fuel and air will not be uniformly mixed, as is typically assumed. Nonuniformity in fuel distribution may be created intentionally or may result from hardware limitations, may be axial or transverse, and may be spatial or temporal, depending on the source. Possible sources of nonuniform fuel distribution include, but are not limited to, combustion products/fresh charge buffering (frequently referred to as purge), engine throttling, emissions control, wall heat transfer control, detonation wave shape control, air and fuel valve transients, and nonuniform inlet airflow.

The study that follows is an analysis of the effects of moderate fuel distribution nonuniformities on detonation tube thrust performance (specific impulse I_{sp}). Kailasanath et al.[8] studied the performance effects of unfueled volumetric purge fraction, alternately referred to as partial fill, showing an increase in I_{sp} with increasing purge fraction (decreasing fill fraction), a result confirmed experimentally by Schauer et al.[9] The study of Kailasanath et al.[8] was conducted using a transversely uniform stoichiometric mixture of ethylene and air in the fueled portion of the tube, leaving the purge air at the exit end of the tube unfueled. No spatial transition (gradient) in equivalence ratio was used between the two regions. Purge fractions of up to 80% were studied. However, this approach simultaneously changed the fuel distribution within the tube and the overall equivalence ratio. In another numerical study, Cambier and Tegner[10] examined a variety of issues affecting detonation tube performance, including transverse fuel distribution effects, but, as in the study by Kailasanath et al.,[8] in a manner that simultaneously changed overall equivalence ratio with fuel distribution. Brophy et al.,[11] reported a significant impact in performance from poor transverse fuel distribution in a liquid JP-10 fueled multicycle PDE. However, this qualitative result is for a fairly large variation in fuel distribution caused by an underperforming fuel injector in a less detonable fuel/air mixture that resulted in a failure to propagate the detonation. The current study builds on and expands the consideration of fuel distribution effects by looking at the effects of various axial equivalence ratio gradients, transverse equivalence ratio gradients, and partial fills while maintaining constant overall equivalence ratios. The numerical results are intended to be comparative in nature, looking for trends and relative magnitude effects between the different cases.

Problem Formulation

Computation Domain

The geometry of a detonation tube is generally simple outside of the detonation initiation section upstream of the main detonation chamber. Although the geometry of the detonation initiation section

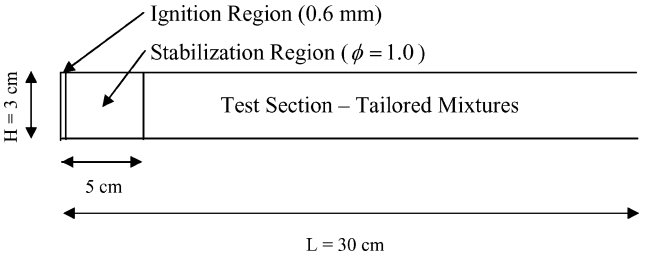

Fig. 1 Geometry for numerical study.

is critical to the operability of the device, this study is confined to the constant-area main detonation chamber. This region represents the majority of the volumetric capacity and, therefore, energy release within the device, making it the dominant region in terms of thrust performance. To keep the geometry as simple as possible, the inflow plane (main air inlet valves) will be modeled as a solid wall, simulating a transitioned detonation with the inlet valves closed.

Typical proof-of-concept PDE detonation tubes being used today are on the order of 5–15 cm in diameter and 100–300 cm in overall length (including the detonation initiation section). For this study, a height of 3.0 cm and a length of 30.0 cm will be used to limit the computational time required. This basic two-dimensional geometry is shown in Fig. 1.

Assumptions

A number of simplifying assumptions are made in this study relative to the actual PDE cycle, as follows.

Deflagration to Detonation Transition

No attempt is made to model the deflagration to detonation transition (DDT) process because the phenomena under study are primarily concerned with steady-state detonation propagation. As shown in Fig. 1, the initiator tube itself is not modeled, nor is any area change from the initiator to the main chamber modeled. A successfully transitioned detonation wave is numerically initiated through the imposition of a high-temperature, high-pressure ignition zone at the left-hand (inflow) side of the domain in a 5.0-cm initiation/stabilization region. The high-pressure, high-temperature ignition zone is set uniformly to 150 atm, 4000 K, and is the full height of the tube, but only 0.6 mm long, with a composition of 25.5% H_2O and 74.5% N_2 by weight. This initiation method is similar to the one employed in Ref. 7. However, whereas Kailasanath and Patnaik used 2% of the total tube volume for the high-temperature/pressure region, only 0.2% is used herein. Therefore, less energy for ignition is applied in this work than that of Ref. 7. The total energy contained in the ignition region is 335 J, which is approximately 1.3% of the heat release from the full 30-cm detonation tube when it is uniformly, stoichiometrically fueled (26.2 KJ). The remaining 4.94-cm stabilization region is maintained as a uniform, stoichiometric unburned quiescent mixture at 1 atm and 300 K for each case to aid in establishing a successful detonation regardless of test case mixture properties. Although this detonation may be initially overdriven to ensure propagation, it equilibrates to near the equilibrium Chapman–Jouget condition by the end of the stabilization zone. This detonation initiation scheme represents a small level of offset in the final specific impulse results. However, the offset should be constant across all of the cases considered and, therefore, has no impact on the trends observed.

Partial Cycle

Only the detonation propagation and blowdown portions of the full PDE cycle are modeled. It is assumed that the purge and refresh cycles are identical for each case. Whereas this might not be rigorously true in practice, such differences would not be expected to be of significant importance. It is further assumed that the blowdown of the tube is complete when the tube exit velocity reaches zero anywhere along the exit plane. In a real cycle, some backflow is likely to occur due to the subambient pressure in the tube from the last reflected expansion wave. This portion of the cycle is important when modeling the filling of the tube, both in terms of the fill time and the performance penalty, but this issue is beyond the scope of this study.

Fuel–Air Combinations

A stoichiometrically fueled 5.0-cm detonation initiation section is used to provide a stabilized detonation wave to the test section. The test section equivalence ratio is varied in either the X direction (axial) or the Y direction (transverse) from case to case. Three test section average equivalence ratios, denoted herein as Φ, are used, one stoichiometric (cases 1–5), one fuel lean (cases 6–9), and one fuel rich (cases 10–13). Nonstoichiometric equivalence ratios of 0.9 and 1.1 were selected, representative of moderate levels of nonuniformity, but still well within expected stable detonation limits throughout the detonation tube. Different buffers or gradients of fuel–air mixture are used to achieve the desired average test section equivalence ratio. Transverse gradient cases are representative of a tube centerline fuel injection configuration, whereas axial gradient cases are representative of a nonconstant tube filling process brought on by time-varying tube inlet and exit conditions. Partial fill cases are representative of fuel lead (H_2 buffer) or fuel lag (air buffer) injection timing. Baseline uniformly fueled cases are used to normalize the results of the subsequent cases. For all cases investigated herein, the unburned mixture is at 1 atm and 300 K and is initially at rest.

Figures 2 and 3 show the different axial and transverse fuel distribution schemes to be used in the test section of the detonation tube, excluding the baseline uniformly fueled cases (cases 1, 6, and 10) and the partial fill cases (cases 9 and 13).

Test cases performed using the opposite orientation of fuel distribution nonuniformity (transverse distributions that were fuel lean at

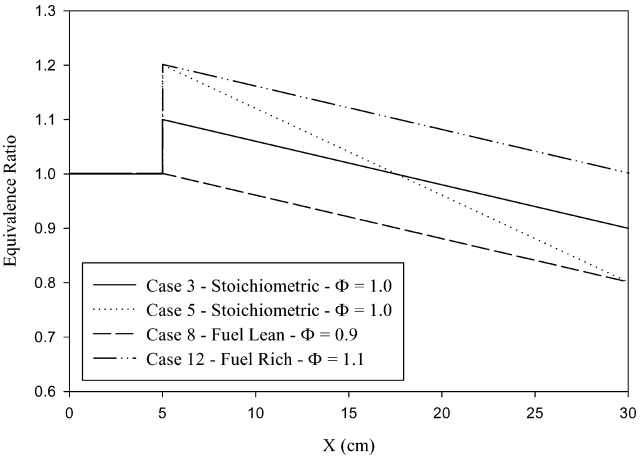

Fig. 2 Test section axial fuel distributions.

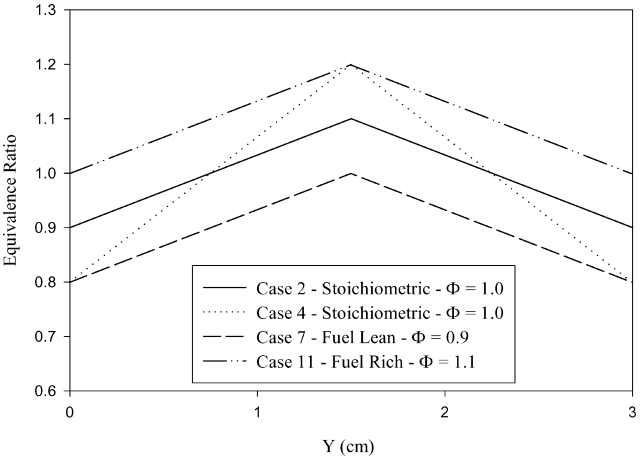

Fig. 3 Test section transverse fuel distributions.

the centerline and fuel rich at the walls and axial distributions that increased in equivalence ratio along the length of the tube instead of decreasing) yielded nearly identical detonation tube performance results as the cases shown and so are not reported in this study.

Numerical Approach

The numerical tool chosen for this study is the SPARK two-dimensional Navier–Stokes code previously developed at the NASA Langley Research Center. The SPARK family of codes was developed primarily for the study of high-speed reacting flows, particularly those found in scramjet engines, and have been used in a number of supersonic combustion and detonation studies.[12–15] The governing equations are solved using a MacCormack fully explicit predictor–corrector scheme that is second-order accurate in space and second-order accurate in time. SPARK has been previously described in detail by Drummond,[16] and so further description will be omitted here. Before applying SPARK to the subject study, additional validation cases were run to verify the performance and accuracy of the code for this application. Detailed comparisons were made to a classical one-dimensional Zel'dovich-Von Neumann-Doring (ZND) solution, as well as to a standing oblique detonation solution (see Ref. 15), which have been documented in Ref. 17. Good quantitative agreement was achieved for each test case.

Detailed Chemistry

Following the work of Cambier and Adelman[18] and Lynch and Edelman,[19] a 7-step, 7-species hydrogen–air detailed chemical mechanism was chosen for this study instead of the more standard 18-step, 9-species mechanism of Jachimowski.[20] For computational efficiency, it is desirable to utilize the simplest possible mechanism that can, with reasonable accuracy, provide the correct time evolution and chemical composition of the detonation wave and the resultant combustion products. The 7-step mechanism is a simple reduction of the 18-step mechanism through the elimination of HO_2 and H_2O_2 from the chemical system, leaving H_2, O_2, H_2O, OH, H, O, and N_2 (inert). This simplification can be justified when it is considered that, in the basic ZND detonation model, ignition occurs after the leading shock, at which point the flow temperature is elevated to a point where the chemistry of HO_2 and H_2O_2 are of less importance.

Figures 4–6 show a comparison of the one-dimensional ZND profiles of pressure, temperature, and H_2O mass fraction calculated using the 7-step kinetic mechanism and the full 18-step mechanism, for a stoichiometric H_2–air mixture initially at 1-atm pressure and 300 K. A ZND code developed by Shepherd[21] is employed herein. The ZND results begin after the leading shock. An equilibrium code developed by Gordon and McBride[22] is used to determine the equilibrium detonation velocity for input to the ZND calculation. The comparison of ZND structure demonstrates that only minor levels of error are introduced through the simplified 7-step mechanism.

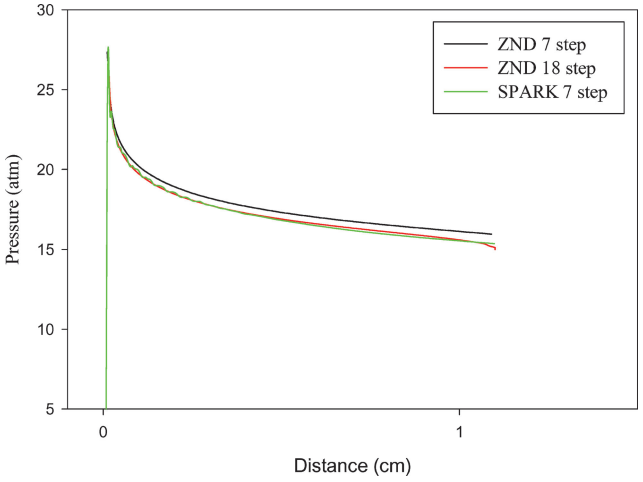

Fig. 4 Comparison of pressure profiles between SPARK and ZND codes.

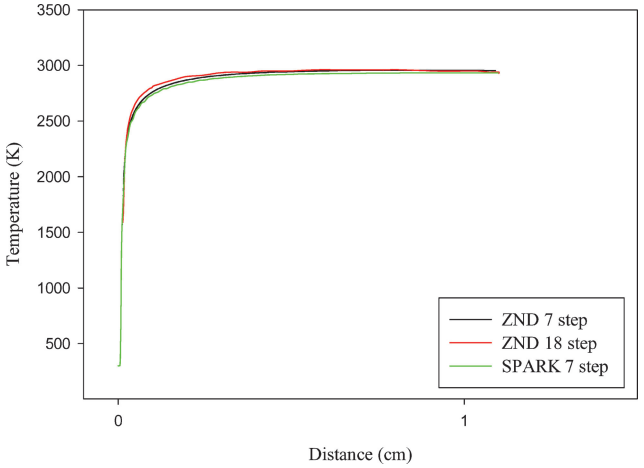

Fig. 5 Comparison of temperature profiles between SPARK and ZND codes.

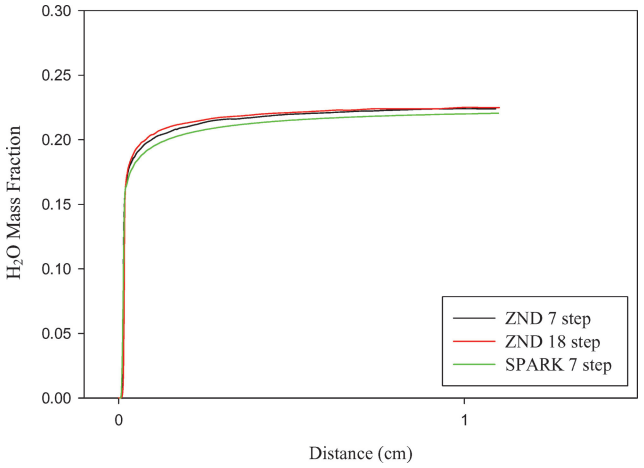

Fig. 6 Comparison of H_2O mass fraction profiles between SPARK and ZND codes.

The SPARK results of the baseline stoichiometric, uniform fuel distribution case (case 1) are also in Figs. 4–6. As shown, the ZND and SPARK results agree very well. The slight differences seen between the results from the different codes are primarily caused by small differences in the thermodynamic data used in each code. However, it is generally apparent that SPARK with the 7-step H_2–air mechanism is adequate for the desired detonation calculations.

Thermodynamic and Transport Properties

SPARK utilizes previously developed analytical expressions for the required thermodynamic and transport properties used throughout the code, which, as with the earlier discussed aspects of the code, have been related in detail in other publications, such as that of Drummond.[16] Species specific heat at constant pressure and species Gibbs energy are calculated using fourth- and fifth-order polynomial curve fits of temperature, respectively. The species laminar viscosity and mixture viscosity are calculated using analytical expressions commonly referred to as Sutherland's law and Wilke's law, respectively. Last, the binary diffusion coefficient and the thermal conductivity are calculated from the Schmidt number (0.22) and Prandtl number (0.72), respectively, which are provided as inputs to the code. All properties were calculated assuming laminar flow throughout.

Computational Grid

The region in the immediate vicinity of the detonation wave front will determine the required physical grid spacing for the computational model. Whereas the thickness of the leading shock

wave is on the order of 1.4×10^{-4} mm (Ref. 23), grid spacing this fine is not typically used for detonation tube performance calculations. A grid spacing in the range of 0.2–1.0 mm has been used in various previously published detonation tube studies.[2,7,24,25] Because the steepest flow and composition variable gradients are expected to be in the axial direction, a relatively coarse grid with a maximum spacing of approximately 1 mm was selected for the transverse grid. The transverse grid spacing was progressively refined near the wall to capture any wall effects that might be discernable from the viscous calculations.

To maintain a reasonable computational time for each case, the total number of grid points was limited to 30,000, resulting in a 300 (axial) × 100 (transverse) point grid. With a tube length of 30 cm, this means that, for any axial grid spacing less than 1 mm, the smallest axial grid spacing would have to be restricted to the region surrounding the reaction zone. This was accomplished for this study by starting with a uniform 300-point axial grid at the smallest grid spacing. As the detonation wave approaches the right-hand edge of the computational domain, the grid is stretched by approximately 30 times the fine grid spacing at the left-hand side, where the reaction has already occurred, lengthening the overall axial domain. The wave structure is, thus, always maintained within the fine grid section, which is effectively shifted to the right every time the detonation wave travels 30 times the fine grid spacing, equivalent to approximately 80 time steps on average. The current result is then linearly interpolated onto the new grid, and the calculation is continued. Once the desired length of the full detonation tube is reached, the fine grid is maintained at the right-hand (exit) end of the tube. Figure 7 shows typical axial grid spacing distributions at three different domain lengths during a calculation using the finest axial grid resolution of 0.01 mm. The corresponding transverse grid spacing distribution is in Fig. 8, with the finest grid resolution of 0.005 mm near the wall.

To determine the detonation zone axial grid spacing required for a grid-independent solution in terms of detonation tube I_{sp}, a grid-refinement study was conducted. A representative nonuniform mixture, corresponding to case 2 (Fig. 3) in the main study, was selected

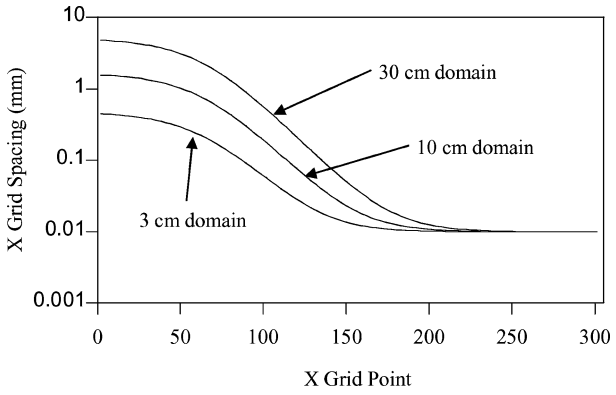

Fig. 7 Axial grid spacing distributions.

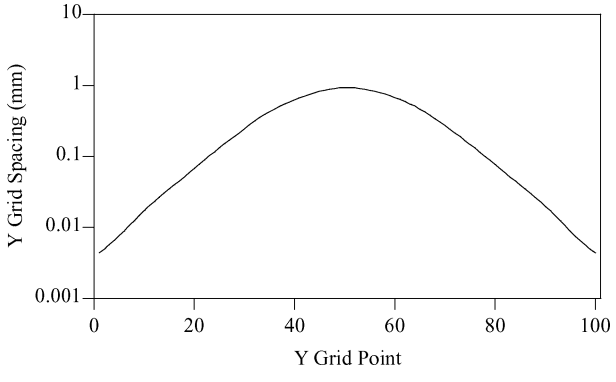

Fig. 8 Transverse grid spacing distribution.

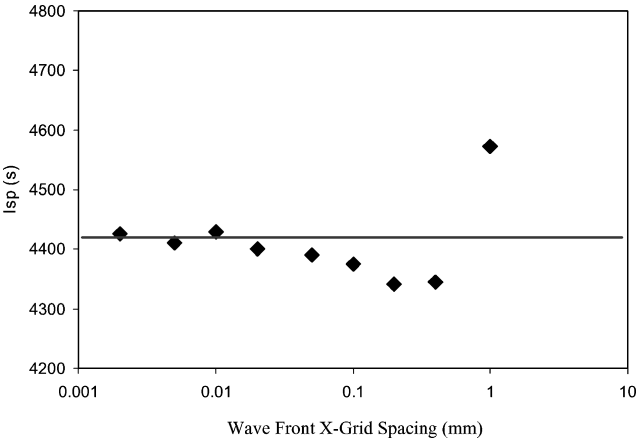

Fig. 9 Detonation tube specific impulse as function of finest axial grid spacing.

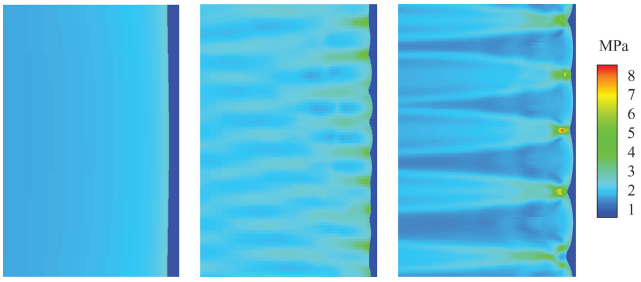

a) b) c)

Fig. 10 Two-dimensional pressure contours of 1 cm high by 0.6 cm long section of computational domain containing detonation wave front for finest axial grid spacings of a) 0.01 mm, b) 0.005 mm, and c) 0.002 mm.

for the grid-resolution study because it would be expected to show more spatially varying flow features and, therefore, more grid dependence, than a uniformly fueled case. Using the transverse grid spacing shown in Fig. 8, axial grid spacings from 1.0 mm down to 0.01 mm were run. The results are compared in Fig. 9, demonstrating reasonable convergence (~4420 s) at the lower end of this range.

To increase the level of assurance that a grid-independent solution had been reached, two additional cases were run with the finest axial grid spacings of 0.005 and 0.002 mm, also shown in Fig. 9. For these two cases, the transverse grid was altered to a uniform grid spacing of 0.1 and 0.05 mm, respectively. This was done to better capture the detailed two-dimensional detonation structure, which was expected to be discernable at that grid resolution, and to avoid numerical difficulties associated with an overly high grid aspect ratio. Although this resulted in a somewhat coarser grid at the wall, this was deemed acceptable because only minimal wall effects had been observed earlier. Whereas the specific impulse remained essentially constant for these additional test cases, detailed field structure became visible. Figure 10 shows the emerging detonation structure in terms of pressure as a function of grid spacing for the three finest axial grid resolution cases at the detonation tube centerline just before the detonation wave passing out of the tube.

Because increasingly refined grid spacings below 0.01 mm did not affect the calculated I_{sp}, but did increase the computational time by as much as an order of magnitude, the 0.01-mm finest grid spacing (Fig. 7) with the varying transverse grid (Fig. 8) was selected for this study. This configuration yielded an average time step based on the fastest reaction time of approximately 3×10^{-9} s.

Boundary Conditions

The left-hand, top, and bottom walls of the two-dimensional detonation tube are all treated as impermeable, dictating that the pressure derivative, the species concentration derivatives, and the

normal component of velocity be set to zero at each wall. No-slip and adiabatic conditions are set at each surface by setting the parallel component of velocity and the temperature derivative to zero.

The tube exit boundary conditions for this type of calculation have been a source of considerable study, with various approaches having been used by different individuals, such as Kailasanath and Patnaik[7] and Wilson and Paxson.[26] The approach of Wilson and Paxson[26] for long detonation tubes ($L/H > 7$) was followed in this study, wherein the supersonic and choked flow conditions present during the first part of the tube blowdown preclude any effect from the decaying blast wave outside the tube on the tube internal flow. Once the tube pressure has dropped sufficiently for the exit to be unchoked, the blast wave is far enough away from the exit to be of no further concern. The supersonic and choked flow boundary conditions were extrapolated from interior grid points, and the methodology of Poinsot and Lele[27] was used for the characteristic subsonic reflecting outflow boundary condition. Each exit grid point was checked at each time step to determine which boundary condition was required.

Computational Results

Before the examination of the detonation tube performance results, it is of value to look at some typical results in detail to further establish the accuracy and stability of the calculations, as well as the general characteristics of the flowfield generated by the detonation process. Figure 11 shows the tube centerline detonation wave speeds for cases 1–3, the first three overall stoichiometric cases. These wave speeds can be compared to the equilibrium Chapman–Jouget wave speeds of 1923 m/s for a uniform equivalence ratio of 0.90, 1969 m/s for a uniform stoichiometric equivalence ratio, and 2005 m/s for a uniform equivalence ratio of 1.10, as calculated using the NASA John H. Glenn Research Center CEA code.[22] The initial overshoot results from the high-pressure, high-temperature detonation initiation process that is overdriven to ensure a well-established detonation in the test section. The change in detonation wave speed at approximately 0.02 ms is caused by the wave exiting the uniformly fueled detonation stabilization zone and entering the test mixture. Case 1, the uniform mixture case, asymptotically approaches the stoichiometric Chapman–Jouget wave speed, achieving a wave speed of 1953 m/s before exiting the detonation tube. Case 2, the transversely varying mixture, initially responds to the higher equivalence ratio along the tube centerline on entering the test section before settling back to follow the same wave speed characteristic as case 1. Case 3, the axially varying mixture, accelerates upward toward the Chapman–Jouget wave speed corresponding to a uniform equivalence ratio of 1.10 as the wave enters the test section, then falls off linearly in direct correlation to the change in test section equivalence ratio. The case 3 wave speed always stays just below the equilibrium wave speed, exiting the tube at a speed of 1903 m/s. In all cases, final wave speeds within 3% of the corresponding equilibrium value were achieved.

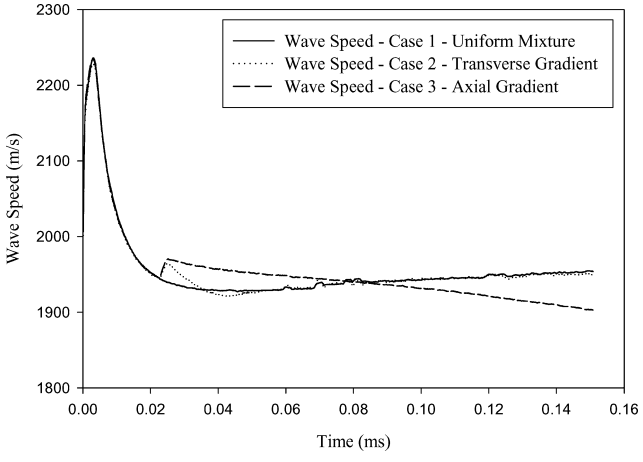

Fig. 11 Detonation wave speeds for average stoichiometric cases 1–3.

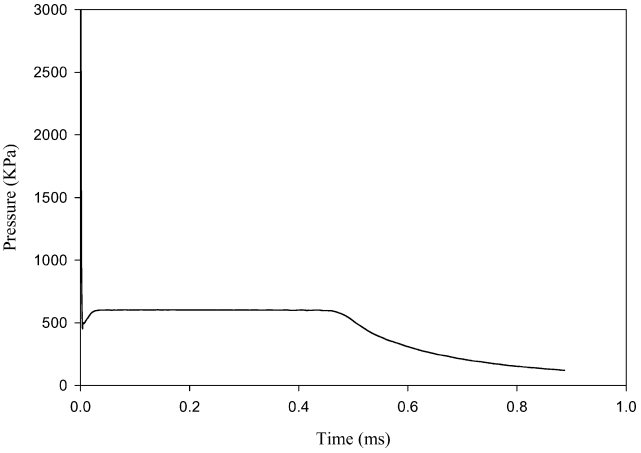

Fig. 12 Detonation tube closed-end pressure for case 2.

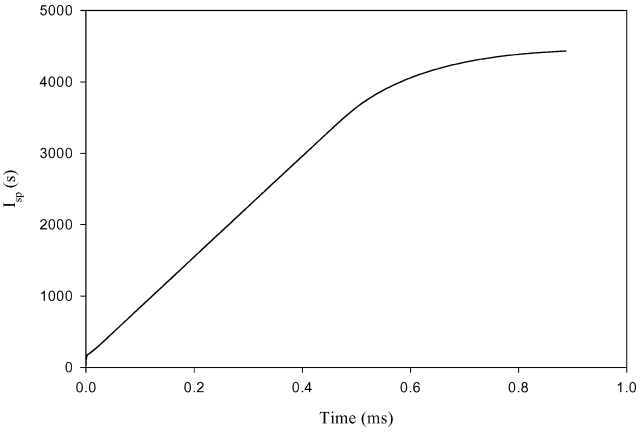

Fig. 13 I_{sp} time history for case 2.

Figures 12 and 13 show the detonation tube closed-end pressure and resulting specific impulse as functions of time for case 2. Figures 12 and 13 show a well-behaved tube blowdown process consistent with previously published results.[7] The final specific impulse of 4429 s shown in Fig. 13 compares reasonably well with the computational results of Kailasanath and Patnaik[7] (4850 s) and the experimental results of Schauer et al.[9] (4000 s), for a stoichiometrically fueled H_2–air detonation tube. The difference in specific impulse from the former study is primarily due to higher initiation energy used by Kailasanath and Patnaik[7] and from the latter study can be attributed to the internal drag resulting from the use of Shchelkin spiral for detonation initiation in the experiment.

Furthermore, we can look at the H_2 mass fraction to determine if any significant flow irregularities are occurring during either the detonation wave propagation or tube blowdown. Figure 14 shows the hydrogen mass fraction in the tube at five different times for case 2, which would be expected to show the greatest two-dimensional behavior due to the transverse mixture variation. The first three images are during the detonation propagation, and the last two are during the blowdown. The postdetonation H_2 distribution remains essentially stratified throughout the entire propagation and blowdown, with the composition distribution at the left of the tube stretching to the right to fill the tube as the blowdown progresses. The products of the uniformly fueled stoichiometric stabilization zone eventually push out most of the stratified combustion products by the end of the simulation. The relatively high levels of residual H_2 at the left-hand (closed) end of the tube seen in this time sequence are a result of the thermal breakdown of H_2O in the high-pressure, high-temperature region used to initiate the detonation and are not a product of the detonation process itself. These results are again typical of all of the test cases run in this study, both for transversely and axially varying mixtures.

Table 1 Summary of test case performance results

Case number	Overall stoichiometry	Type of distribution	Final I_{sp}, s
1	Stoichiometric	Uniform	4450
2	Stoichiometric	Transverse $\phi = 0.9$–1.1	4429
3	Stoichiometric	Axial $\phi = 0.9$–1.1	4459
4	Stoichiometric	Transverse $\phi = 0.8$–1.2	4410
5	Stoichiometric	Axial $\phi = 0.8$–1.2	4440
6	Fuel lean	Uniform	4706
7	Fuel lean	Transverse	4699
8	Fuel lean	Axial	4722
9	Fuel lean	Partial fill (air)	4676
10	Fuel rich	Uniform	4177
11	Fuel rich	Transverse	4168
12	Fuel rich	Axial	4175
13	Fuel rich	Partial fill (H_2)	4204

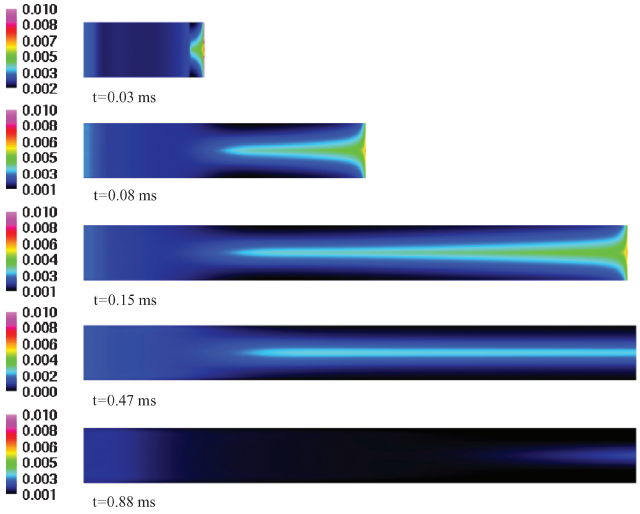

Fig. 14 Two-dimensional H_2 mass fraction distributions for case 2, transverse gradient.

Moving on to the performance results, Table 1 summarizes the final specific impulse results of the 13 cases run in this study, with ϕ referring to the local equivalence ratio within the detonation tube. Several comparisons can be made to illuminate the effects of fuel distribution and equivalence ratio.

When the cases within each average equivalence ratio grouping are compared, note that the case-to-case variation in specific impulse is less than 1%. Although there is some trending within the results, for example, transversely varying mixtures performing slightly worse in all cases, the level of variation in performance should be considered negligible.

When the uniform mixture baseline cases 6 and 10 are compared with the corresponding partial fill cases 9 and 13, it is seen that there is no particular advantage of partial fill over a uniform mixture with the same overall stoichiometry.

Last, when the results for the uniformly fueled baseline cases 1, 6, and 10 are plotted, as shown in Fig. 15, it is seen that I_{sp} is essentially linear with equivalence ratio in the limited range of equivalence ratios studied herein. Inclusion of the stabilization zone raises the overall equivalence ratio of the fuel lean cases to 0.92 and lowers the overall equivalence ratio of the fuel rich cases to 1.08. The linear relationship between specific impulse and equivalence ratio implies that the total impulse is relatively constant, which was in fact the case. Whereas the total mass of detonative mixture in the tube is declining linearly with increasing equivalence ratio, this is offset by an increasing mass-averaged exit velocity due to an increased sound speed in the combusted mixture resulting from the low molecular weight of the additional hydrogen. Thus, the cycle mass-averaged exit momentum for the different equivalence ratios is nearly constant.

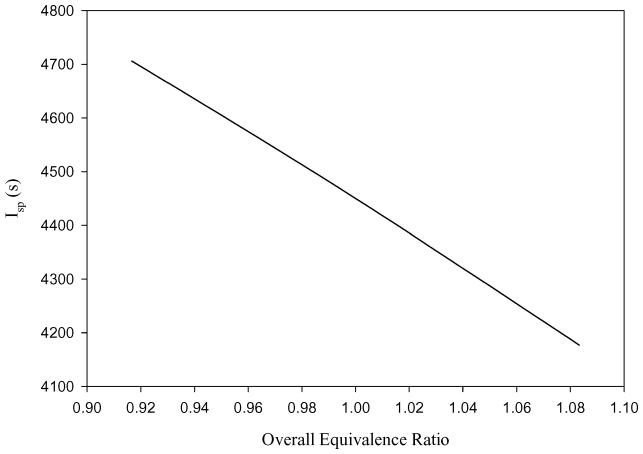

Fig. 15 Final I_{sp} as a function of overall equivalence ratio, including stabilization zone, for cases 1, 6, and 10.

Conclusions

The primary conclusion to be drawn from this study is that a lack of fuel–air mixing up to a moderate level in a hydrogen-fueled airbreathing detonation tube has almost no effect on the thrust performance of the system. Put another way, thrust performance is almost completely independent of combustion efficiency in the vicinity of an overall equivalence ratio of one. This is an encouraging preliminary result for the design of such systems because it appears to be unnecessary to go to extremes to achieve good mixing in the fuel injection process. These results also imply that it is probably unnecessary to match precisely air and fuel valve opening and closing profiles to maintain constant equivalence ratio.

There are a couple of secondary conclusions that may also be drawn for H_2–air systems. First, decreased equivalence ratio and fuel-lag partial filling of the detonation tube are essentially equivalent at the same overall equivalence ratio. If anything, it appears slightly more advantageous to lower the equivalence ratio as long as the mixture remains detonable. Obviously, a point is reached where it is impossible to lower the equivalence ratio and maintain a detonable mixture. At this point, further throttling can be achieved by partially filling the detonation tube with a lean detonable mixture.

Second, transversely and axially varying mixtures remain essentially stratified throughout the detonation propagation and blowdown process. One benefit of this behavior is that it will be possible to qualitatively evaluate mixing within a detonation tube by looking at the temporal and spatial distribution of products coming out of the tube, thus reducing the need for costly optical test sections in detonation tubes. A related conclusion is that one-dimensional simulations are adequate for nontransversely varying mixtures. Because there was minimal mixing or shear effect observed, despite the no-slip condition maintained at the wall, a one-dimensional simulation should capture the principal effects of the detonation propagation and blowdown.

Further analysis is required to determine the effects of fuel heating value and molecular weight (fuel type), as well as the impact of nondetonative fuel–air mixture regions in the detonation tube. Differing trends may be found when these parameters are considered.

Acknowledgments

This analysis was performed under the auspices of the Pulse Detonation Engine Technology Project of the Aerospace Propulsion and Power Program at NASA John H. Glenn Research Center at Lewis Field as part of a Master of Science in Engineering degree program at Case Western Reserve University under the direction of C. J. Sung.

References

[1]Nichols, J., Wilkinson, H., and Morrison, R., "Intermittent Detonation as a Thrust Producing Mechanism," *Jet Propulsion Journal of the American Rocket Society*, Vol. 27, No. 5, 1957, pp. 534–541.

[2]Wu, Y., Ma, F., and Yang, V., "System Performance and Thermodynamic Cycle Analysis of Airbreathing Pulse Detonation Engines," *Journal of Propulsion and Power*, Vol. 19, No. 4, 2003, pp. 556–567.

[3]Kailasanath, K., "Recent Developments in the Research on Pulse Detonation Engines," *AIAA Journal*, Vol. 41, No. 2, 2003, pp. 145–159.

[4]Kailasanath, K., "Applications of Detonations to Propulsion: A Review," AIAA Paper 99-1067, Jan. 1999.

[5]Kaemming, T. A., "Integrated Vehicle Comparison of Turbo-Ramjet Engine and Pulsed Detonation Engine (PDE)," American Society of Mechanical Engineers, ASME Paper 2001-GT-0451, June 2001.

[6]Coleman, M. L., "Overview of Pulse Detonation Propulsion Technology," Chemical Propulsion Information Agency, CPIA Rept. CPTR 70, Columbia, MD, April 2001.

[7]Kailasanath, K., and Patnaik, G., "Pulsed Detonation Engines—What is its Performance," *Proceedings of the 24th JANNAF Airbreathing Propulsion Subcommittee and 36th JANNAF Combustion Subcommittee Joint Meeting*, CPIA Publ. 692, Vol. 1, Chemical Propulsion Information Agency, Columbia, MD, 1999, pp. 131–140.

[8]Kailasanath, K., Patnaik, G., and Li, C., "On Factors Controlling the Performance of Pulsed Detonation Engines," *Control of Detonation Processes*, edited by G. Roy, S. Frolov, D. Netzen, and A. Borisov, Elex-KM, Moscow, 2000, pp. 172–174.

[9]Schauer, F., Stutrud, J., and Bradley, R., "Detonation Initiation Studies and Performance Results for Pulsed Detonation Engine Applications," AIAA Paper 2001-1129, Jan. 2001.

[10]Cambier, J.-L., and Tegner, J. K., "Strategies for PDE Performance Optimization," AIAA Paper 1997-2743, July 1997.

[11]Brophy, C. M., Sinibaldi, J., and Netzer, D. W., "Effects of Fuel Distribution on Pulse Detonation Engine Operation and Performance," International Symposium for Air Breathing Engines, ISABE Paper 2001-1173, Sept. 2001.

[12]Drummond, J. P., and Mukunda, H. S., "A Numerical Study of Mixing Enhancement in Supersonic Reacting Flow Fields," AIAA Paper 88-3260, July 1988.

[13]Drummond, J. P., "A Two-Dimensional Numerical Simulation of a Supersonic, Chemically Reacting Mixing Layer," NASA TM-4055, Dec. 1988.

[14]Carpenter, M. H., "Three-Dimensional Computations of Cross-Flow Injection and Combustion in a Supersonic Flow," AIAA 89-1870, June 1989.

[15]Thaker, A. A., and Chelliah, H. K., "Numerical Prediction of Oblique Detonation Wave Structures Using Detailed and Reduced Reaction Mechanisms," *Combustion Theory and Modelling*, Vol. 1, No. 4, 1997, pp. 347–376.

[16]Drummond, J. P., "Supersonic Reacting Internal Flow Fields," NASA TM-103480, Jan. 1989.

[17]Perkins, H. D., "Effects of Fuel Distribution on Detonation Tube Performance," M.S. Thesis, Dept. of Mechanical and Aerospace Engineering, Case Western Reserve Univ., Jan. 2002; also NASA TM-2002-211712.

[18]Cambier, J.-L., and Adelman, H. G., "Preliminary Numerical Simulations of a Pulsed Detonation Wave Engine," AIAA Paper 88-2960, July 1988.

[19]Lynch, E. D., and Edelman, R., "Computational Fluid Dynamic Analysis of the Pulse Detonation Engine Concept," AIAA Paper 94-0264, Jan. 1994.

[20]Jachimowski, C. J., "An Analytical Study of the Hydrogen–Air Reaction Mechanism with Application to Scramjet Combustion," NASA TP 2791, Feb. 1988.

[21]Shepherd, J. E., "Chemical Kinetics of Hydrogen–Air–Diluent Detonation," *Dynamics of Explosions*, edited by J. R. Bowen, Vol. 106, Progress in Astronautics and Aeronautics, AIAA, New York, 1986, pp. 263–293.

[22]Gordon, S., and McBride, B. J., "Computer Program for Calculation of Complex Chemical Equilibrium Compositions and Applications," NASA RP 1311, Oct. 1994.

[23]Shapiro, A. H., *The Dynamics and Thermodynamics of Compressible Fluid Flow*, Ronald, New York, 1953, pp. 133, 134.

[24]Li, C., and Kailasanath, K., "Partial Fuel Filling in Pulse Detonation Engines," *Journal of Propulsion and Power*, Vol. 19, No. 5, 2003, pp. 908–916.

[25]Tangirala, V. E., Dean, A. J., Chapin, D. M., Pinard, P. F., and Varatharajan, B., "Pulsed Detonation Engine Processes: Experiments and Simulations," *Combustion Science and Technology*, Vol. 176, No. 10, 2004, pp. 1779–1808.

[26]Wilson, J., and Paxson, D. E., "On the Exit Boundary Condition for One-dimensional Calculations of Pulsed Detonation Engine Performance," *Proceedings of the 18th International Colloquium on Detonation, Explosion, and Reactive Systems*, edited by J. R. Borven, Univ. of Washington, Seattle, Washington, July 2001; also Paper No. 182.

[27]Poinsot, T. J., and Lele, S. K., "Boundary Conditions for Direct Simulations of Compressible Viscous Flows," *Journal of Computational Physics*, Vol. 101, No. 1, 1992, pp. 104–129.